

1 **CLAS12 Run-group H Experiments with a**  
2 **Transversely Polarized Target**

3

4 **Abstract**

5 This document provides an update on the physics case and preparatory work for the  
6 C1 conditionally approved CLAS12 deep-inelastic scattering (DIS) experiments with  
7 a transversely polarized target, identified as run-group H. 1

8 **Contents**

|    |     |                                |    |
|----|-----|--------------------------------|----|
| 9  | 1   | <b>Introduction</b>            | 2  |
| 10 | 2   | <b>Physics Highlights</b>      | 2  |
| 11 | 3   | <b>The Transverse Target</b>   | 4  |
| 12 | 3.1 | HDice in electron beams        | 4  |
| 13 | 3.2 | Dynamically polarized target   | 5  |
| 14 | 3.3 | Polarizing magnet              | 6  |
| 15 | 3.4 | Target Figure-of-Merit         | 7  |
| 16 | 4   | <b>The CLAS12 Spectrometer</b> | 9  |
| 17 | 4.1 | <b>Forward Detector</b>        | 9  |
| 18 | 4.2 | <b>Luminosity</b>              | 11 |
| 19 | 5   | <b>Physics Observables</b>     | 12 |
| 20 | 5.1 | <b>Semi-inclusive Physics</b>  | 12 |
| 21 | 5.2 | <b>Exclusive Physics</b>       | 12 |
| 22 | 6   | <b>Summary</b>                 | 12 |

## 1 Introduction

The CLAS12 run-group H (RGH) comprises 3 experiments approved with rating A by PAC39 to run for a total of 110 days with a 11 GeV beam scattering off a transversely polarized target.

- **C12-11-111** *Transverse spin effects in SIDIS at 11 GeV with a transversely polarized target using CLAS12*: a multi-dimensional analysis of the semi-inclusive (SIDIS) reactions to access transversity and tensor charge, and the Sivers and Collins functions connected with the spin-orbit phenomena of the strong-force dynamics [1];
- **C12-12-009** *Measurement of transversity with dihadron production in SIDIS with transversely polarized target*: a multi-dimensional analysis of the SIDIS reactions exploiting the dynamics of the di-hadron final state to access transversity in the benchmark collinear limit and investigate novel parton correlations inaccessible on the single hadron case [2].
- **C12-12-010** *Deeply Virtual Compton Scattering at 11 GeV with transversely polarized target using the CLAS12 Detector*: a multi-dimensional analysis of the DVCS reaction to access the most elusive Generalized Parton Distribution entering the orbital momentum sum rule (Ji sum rule) [3].

The experiments were approved with the C1 condition to address the technical issues related to the target performance with the laboratory management before scheduling [4].

All the three experiments were selected among the high-impact JLab measurements by PAC42 [5].

RGH experiments are precursor of EIC in one of the pillars of its physics program [6]. Distinctive features in common of all the three experiments are the precise measurement of novel parton distributions and phenomena in an unexplored valence region where their magnitude could be maximal, a luminosity at least on order of magnitude higher than the precursor experiments, a large acceptance detector for the disentanglement of the various correlations and kinematic regimes, an excellent particle identification capability to access flavor sensitivity, the development of innovative solutions for the transversely polarized target to reach the best factor of merit and kinematic coverage.

## 2 Physics Highlights

In the recent years, new parton distributions (PDFs) and fragmentation functions (FFs) have been introduced to describe the rich complexity of the hadron structure, focusing on the parton transverse degrees of freedom at the scale of confinement and moving toward the achievement of a 3D description of the parton dynamics. Relevant examples are transverse momentum dependent (TMD) and generalized (GPD) parton distributions, relating the longitudinal (referred

62 to the direction of the hard probe) momentum fraction, with the intrinsic par-  
63 tonic transverse momentum or position, respectively. Their detailed investiga-  
64 tion requires a novel level of sophistication in the deep-inelastic scattering (DIS)  
65 experiments that should conjugate precision, in discriminating semi-inclusive  
66 and exclusive reaction details, and power, in collecting large amount of data to  
67 allow multi-dimensional analyses.

68 **The CLAS12 run-group H program collects several fundamental**  
69 **measurements that provide access to elusive quantities and are only**  
70 **possible with the use of a transversely polarized target in conjunction**  
71 **with a large acceptance high-precision spectrometer.**

72 The **Transversity** PDF describes the parton transverse polarization inside  
73 a transversely polarized nucleon, reflects the relativistic nature of the parton  
74 confinement and exhibits peculiar evolution properties. It is the less known  
75 PDF that does not vanish when integrated in the transverse momentum  $k_{\perp}$ ,  
76 and can thus be studied in the collinear limit. Although essential for the nu-  
77 cleon description, due to its chirally-odd nature transversity has only recently  
78 been accessed in a limited kinematic range and with a large uncertainty that  
79 still prevents a reliable flavor decomposition [7]. Its first moment in Bjorken  
80  $x$ , the tensor charge, is a fundamental quantity in quantum chromodynamics  
81 (QCD) connected to searches of beyond Standard Model phenomena such as the  
82 Electric Dipole Moment (EDM) of particles [8] and the tensor interaction [9].  
83 CLAS12 data will cover an unexplored Bjorken- $x$  interval in the valence region,  
84 providing unprecedented constraints to the tensor charge and allowing precise  
85 comparison with lattice QCD, which has made remarkable progresses in the  
86 past decades [10].

87 The **Sivers** PDF is a genuine TMD function which vanishes with  $k_{\perp}$  in-  
88 tegration. Among the most intriguing parton distributions, it requires a non-  
89 zero parton orbital angular momentum and a correlation with the nucleon spin.  
90 As a consequence of its non-trivial gauge-invariant definition, the Sivers func-  
91 tion probes QCD at the amplitude level: it is naively T-odd (do not violate  
92 T-invariance due to the interaction phase) and exhibits a peculiar process de-  
93 pendence. A sign change is expected when moving from SIDIS to Drell-Yan  
94 processes, whose verification is one of the most urgent goals of the present ex-  
95 perimental activity [7]. It is among the few TMDs that, while describing the  
96 non-perturbative nature when  $k_{\perp} \ll Q^2$ , should in principle match the pertur-  
97 bative regime with increasing transverse momentum, providing a formal bridge  
98 between the two QCD descriptions [11]. CLAS12 data will allow an extended  
99 coverage in the valence region and a disentanglement of the Sivers kinematic  
100 dependences, a crucial information for the study of these phenomena and the  
101 connections among different QCD regimes.

102 The **Collins** and **Di-hadron** FFs originate from spin-orbit effects connect-  
103 ing the spin of a fragmenting quark with the final observed hadron or di-hadron  
104 transverse momentum, respectively. Convincing evidences have been found for  
105 the existence of these mechanisms [7]. These peculiar FFs act as a polarime-

106 ter and allow to access the elusive chirally-odd distribution functions in SIDIS  
107 reactions. In particular the Di-hadron FF, sensitive to the hadron pair *relative*  
108 transverse momentum, can be studied in the collinear limit providing a comple-  
109 mentary access to transversity that does not depend on the TMD formalism,  
110 and can be reliably extended to the hadron-hadron scattering case [12]. High  
111 precision data from CLAS12 can complement present and future information  
112 gathered at the much higher center-of-mass energy of experiments at the  $e^+e^-$   
113 colliders, like BELLE-II [13], and at hadron-hadron colliders, like PHENIX and  
114 STAR [14].

115 The **GPD E** describes asymmetries in the parton spatial distribution that  
116 imprint the underlying confinement dynamics. It is the least known GPD that  
117 enters the Ji sum rule quantifying the parton orbital momentum [15]. Its mea-  
118 surement in the golden deeply-virtual Compton scattering (DVCS) channel re-  
119 quires a transversely polarized proton target as a complementary approach to  
120 the beam spin asymmetry off an unpolarized neutron target [16]. As the latter  
121 is among the goals of RGB experiments that already took data, both mea-  
122 surements can be accomplished at CLAS12 providing an unprecedented level of  
123 information.

### 124 **3 The Transverse Target**

125 The original target proposed for the Run Group H experiments was HDice, a  
126 frozen spin target of polarized solid hydrogen deuteride. However, it has been  
127 determined that this target system is not suitable for use in electron experi-  
128 ments, and so we will instead utilize a technology that has been successfully  
129 implemented in numerous experiments at Jefferson Lab, Dynamic Nuclear Po-  
130 larization (DNP). This technique provides a number of advantages over the  
131 initial choice, including significantly higher polarization and much greater re-  
132 sistance to the depolarizing effects of the electron beam. Its drawbacks are  
133 target molecules with a greater fraction of unpolarized nucleons and a reliance  
134 on higher field, higher-uniformity magnets. Our decision is explained below.

#### 135 **3.1 HDice in electron beams**

136 As in all frozen spin targets, the nuclear spins in HDice are polarized in a high  
137 magnetic field and then placed in a lower field for data taking. During the  
138 experiment the polarization decays in an exponential manner towards a small,  
139 thermal equilibrium polarization governed by the sample temperature  $T$  and  
140 holding field  $B$ . The rate of this decay is characterized by the spin-lattice re-  
141 laxation time  $T_1$ , which is also a strong function of both temperature and field.  
142 The relaxation time is also strongly affected by the presence of paramagnetic  
143 impurities within the sample. In fact, paramagnetic impurities are the domi-  
144 nant source of nuclear spin relaxation in most dielectric solids, and it is these  
145 impurities that eliminate HDice as a viable target for Run Group H.

146 Although the HDice concept dates to 1967 [17], its use in particle experi-  
147 ments has not been widespread and limited to two low-luminosity experiments  
148 with beams of real photons [18, 19]. Tests performed with charged particles have  
149 been discouraging, as HD samples with initially long relaxation times rapidly  
150 lost their polarization due to the radiolytic production of paramagnetic species  
151 in the material (predominately atomic H and D), combined with beam heat-  
152 ing. At the Cornell Synchrotron, the relaxation time of a polarized HD sample  
153 dropped from 8 hours to 15 minutes after 22 minutes of exposure to a pulsed  
154 beam of 10 GeV electrons with an equivalent current of 10 nA. In 2012 at Jef-  
155 ferson Lab, tests were performed in Hall B with a 6 GeV electron beam. In the  
156 most prolonged exposure, an HD sample with  $T_1 > 700$  hours lost 98% of its  
157 polarization after 14 hours at 1 nA.

158 A series of detailed measurements were again performed at JLab using 8 MeV  
159 electrons from the Upgraded Injector Test Facility (UITF). A number of modi-  
160 fications were made to address shortcomings of the previous tests: the magnetic  
161 holding field was increased from 0.3 T to 1.0 T, the sample was redesigned  
162 for improved heat removal, the beam current was reduced to 0.25 nA to main-  
163 tain a lower sample temperature, and the beam raster frequency was increased  
164 from 1 Hz to 1000 Hz to minimize localized heating. Despite these efforts,  
165 the polarized sample was reduced to 37% ( $1/e$ ) of its initial polarization af-  
166 ter approximately  $3.7 \times 10^{13} \text{ e}^- \text{ cm}^{-2}$ , corresponding to an average  $T_1$  of about  
167 2 hours at  $1 \text{ nA cm}^{-2}$ . It was also observed that the rate of polarization loss  
168 increased with accumulated dose and decreased when the heat from the beam  
169 was removed. Both are hallmarks of spin relaxation due to beam-induced para-  
170 magnetic impurities.

## 171 3.2 Dynamically polarized target

172 A more common and powerful alternative to HDice is dynamically polarized  
173 solid ammonia,  $\text{NH}_3$  and  $\text{ND}_3$ . These polarized materials have been successfully  
174 utilized on multiple occasions at Jefferson Lab, with beam currents up to 140 nA  
175 [21], and with in-beam proton and deuteron polarizations exceeding 90% and  
176 50%, respectively. One key to this material's success at Jefferson Lab is the  
177 fact that the paramagnetic impurities responsible for depolarizing frozen spin  
178 targets are actually used to dynamically *polarize* ammonia's nuclear spins.

179 In the case of ammonia, the amino radicals  $\dot{\text{N}}\text{H}_2$  and  $\dot{\text{N}}\text{D}_2$  are produced at  
180 concentrations of about  $10^{-4}$  in the solid lattice by irradiation with an electron  
181 beam prior to the scattering experiment. These radicals are stable at temper-  
182 atures below about 100 K, and so the samples can be indefinitely stored under  
183 liquid nitrogen until needed. Each radical has a single, unpaired electron whose  
184 spin can be highly polarized in more modest field and temperature conditions  
185 than those required for nuclear polarization. For example, at the 5 T, 1 K  
186 conditions of most JLab targets, the electron polarization exceeds 99% while  
187 the proton polarization is only 0.5%/. This high electron polarization is then  
188 transferred to the nuclear spins using microwave-induced transitions in which  
189 both the electron and nuclear spins flip simultaneously. The nuclear polarization

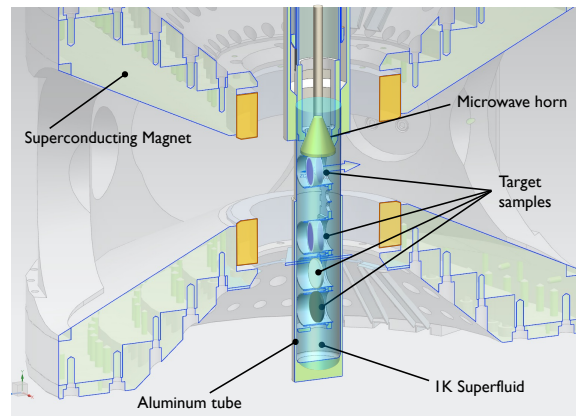


Fig. 1: Standard configuration of a target ladder for a DNP target system. Multiple samples (ammonia, carbon, polyethylene, empty, etc) are suspended in a bath of 1 K superfluid at the center of the polarizing magnet.

190 typically reaches its maximum value in less than two hours and can be selected  
 191 to be positive or negative by adjusting the microwave frequency slightly below  
 192 or above the electron spin resonance frequency.

193 During the scattering experiment, additional radical species such as atomic  
 194 hydrogen are produced that are stable at the target's operating temperature of  
 195 1 K. These do not contribute to the dynamic polarization process, but do cause  
 196 spin relaxation at an ever-increasing rate. This "radiation damage" is typically  
 197 repaired after a dose of about  $5 \times 10^{15} \text{ e}^- \text{cm}^{-2}$  by annealing the sample at  
 198 90 K for several minutes. Assuming a 2 nA beam current and 1.5 cm target  
 199 diameter, this dose will be accumulated after approximately one week of beam  
 200 time. More than one ammonia sample can be included on the target ladder,  
 201 further increasing the time between anneals. With two ammonia samples, the  
 202 overhead needed for the annealing process will be about 2–3%. Carbon and  
 203 polyethylene samples can also be included on the ladder for dilution studies  
 204 (Fig. 1).

### 205 3.3 Polarizing magnet

206 An obvious challenge to the operation of any transversely polarized target in  
 207 Hall B is the *longitudinal* field produced by the CLAS12 solenoid. The original  
 208 Run Group H proposals describe a solution using three sets of coils around the  
 209 HDice target: a combination of solenoid and Helmholtz coils to negate the field  
 210 of the CLAS12 solenoid, and saddle coils to generate a 0.5–1 T field in the  
 211 vertical direction.

212 More recently, the use of the bulk superconductor magnesium diboride ( $\text{MgB}_2$ )  
 213 has been explored. In this scenario, a hollow tube of  $\text{MgB}_2$ , surrounding the  
 214 target sample, is cooled below its critical temperature while exposed to an ex-

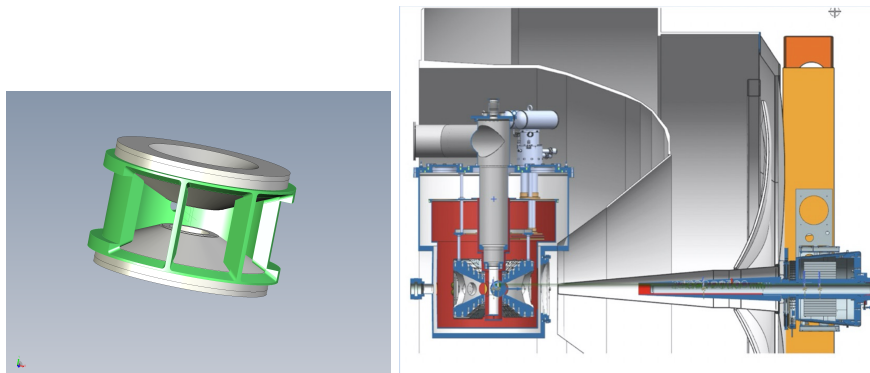


Fig. 2: Left: 3D model of the 5 T split-coil magnet for Run Group H. The opening in the forward directions for scattered particles spans  $\pm 60^\circ$  in the horizontal plane and  $\pm 25^\circ$  in the vertical. Right: Conceptual design showing the dynamically polarized target at the center of the CLAS12 HTCC.

215 ternal magnetic field transverse to the tube's axis. Upon removal from the  
 216 external field, electrical currents are naturally generated within the supercon-  
 217 ducting walls to maintain the original transverse field in the tube's interior. As  
 218 the target cryostat is moved into the CLAS12 solenoid, the internal currents  
 219 again adjust to maintain the transverse field. A test program at INFN Fer-  
 220 rara has shown very promising results [30, 31], but the technology is not yet at  
 221 the level of maturity needed for Run Group H. For example, it is not known  
 222 if the technique can maintain the uniform, constant field needed for dynamic  
 223 polarization.

224 In this document, we instead take a more simple and direct approach to the  
 225 problem. The CLAS12 solenoid will be replaced by a superconducting, split-coil  
 226 magnet similar to those previously used to polarize targets at JLab. The new  
 227 coil will produce a 5 T field in the vertical direction and feature an opening that  
 228 spans  $\pm 60^\circ$  in the horizontal plane and  $\pm 25^\circ$  in the vertical. A preliminary  
 229 model of the magnet, as well as a conceptual design of the target cryostat inside  
 230 the CLAS12 HTCC are shown in Fig. 2.

### 231 3.4 Target Figure-of-Merit

232 We can compare the new target design with the original HDice option by defining  
 233 a figure-of-merit that reflects the time required to achieve a certain statistical  
 234 precision in the measured scattering asymmetries:

$$\text{FoM} = \mathcal{L}(1 - \tau)f^2P^2 \quad (1)$$

235 Here  $\tau$  is the overhead needed for routine target operations,  $f$  is the target  
 236 dilution factor, and  $P$  is the average target polarization. The luminosity  $\mathcal{L}$  is

| Quantity                     | HD   | NH <sub>3</sub> |
|------------------------------|------|-----------------|
| (1- $\tau$ )                 | 0.90 | 0.97            |
| $f$                          | 1    | 3/17            |
| $P$                          | 0.25 | 0.85            |
| $I$ (nA)                     | 1.0  | 2.0             |
| $\rho$ (g/cc)                | 0.10 | 0.87            |
| $x$ (cm)                     | 1.3  | 1.0             |
| $\mathcal{L} \times 10^{33}$ | 0.5  | 5.0             |
| FoM $\times 10^{31}$         | 2.8  | 11.4            |

Tab. 1: Comparison of solid HD and NH<sub>3</sub> as polarized target materials. The density of the materials has not been corrected for the aluminum wires used to cool solid HD ( $\sim 20\%$  by weight) or the superfluid helium that cools solid ammonia ( $\sim 10\%$  by weight). Details in the text.

237 the product of the beam intensity  $I/e$  and target thickness in nuclei per square  
238 centimeter:

$$\mathcal{L} = \frac{I}{e} \rho x N_A \quad (2)$$

239 In dynamically polarized NH<sub>3</sub>, the overhead is dominated by the annealing  
240 process (3%), the dilution factor for polarized protons is 3/17, and an average  
241 polarization of 0.85 is assumed. This polarization was demonstrated during a  
242 6 GeV experiment in Hall A using a polarized target similar to the one described  
243 here and a 10 nA beam current [22]. The luminosity will not be limited by  
244 the target operation in this case, but by the background produced by Moeller  
245 scattering. In Sec. 4.2 we argue that a conservative value is  $5 \times 10^{33} \text{ cm}^{-2}\text{s}^{-1}$ .  
246 This corresponds to about 2 nA impinging on a 1 cm long NH<sub>3</sub> target.

247 For HDice we choose values under the assumption that the system could have  
248 successfully satisfied the criteria imposed by PAC-42: a polarization lifetime of  
249 500 hours in a 1 nA beam. For initial proton and deuteron polarizations of 0.6  
250 and 0.15, respectively, the mean nuclear polarization during a 500 h lifetime will  
251 be 0.25. It is not possible to repolarize the HD sample on the Hall B beamline.  
252 Instead, it must be replaced with a fresh sample, which takes about two days.  
253 This corresponds to an overhead of 10%. The length of the target chosen for the  
254 UITF test was 1.3 cm, and with a density of 0.10 g/cm<sup>3</sup>, giving a luminosity of  
255  $5 \times 10^{32} \text{ cm}^{-2}\text{s}^{-1}$ . The results are given in Table 1 and indicate the NH<sub>3</sub> target  
256 has a figure-of-merit four times greater than HD.



## 257 4 The CLAS12 Spectrometer

258 The CLAS12 spectrometer has been designed to run at high luminosity, up to  
 259 about 3 orders of magnitude larger than the precursor experiments like HER-  
 260 MES and COMPASS, and bring the 3D nucleon structure study into the preci-  
 261 sion phase. CLAS12 started the data-taking with unpolarized hydrogen targets  
 262 in spring 2018 and has so far successfully run with different targets and detec-  
 263 tor configurations. In particular, CLAS12 successfully ran with longitudinally  
 264 polarized  $\text{NH}_3$  and  $\text{ND}_3$  targets. Detailed calibration procedures and event re-  
 265 construction algorithms have been developed to reach a performance close to,  
 266 or in some cases superior to, the design specifications.

### 267 4.1 Forward Detector

268 With respect to the goals of run-group H, the spectrometer has specifically demon-  
 269 strated to be able to achieve the following performance.

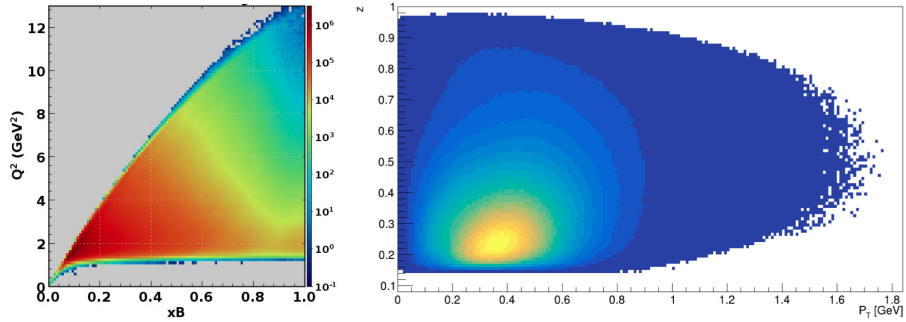


Fig. 3: (Left) The CLAS12 reach in the relevant kinematic variables at a beam energy of 10.6 GeV. (Left) Inclusive electron coverage in the hard scale  $Q^2$  versus Bjorken  $x$ . (Right) Charged hadrons coverage in the transverse momentum  $P_T$  versus the fractional energy  $z$ .

270 **Tracking** The single track reconstruction efficiency has been improved with  
 271 the implementation of ML algorithm to support effective denoising and track  
 272 segment finding, to a level of better than 90% at the design luminosity of  $10 \times 10^{35}$   
 273  $\text{cm}^{-2}\text{s}^{-1}$ , with a dependence of  $98\% - 0.1 \times I$  in nA of beam current. The typical  
 274 measured resolutions in the relevant kinematic quantities are  $\Delta p/p = 0.67\%$ ,  
 275  $\Delta\theta = 0.85$  mrad and  $\Delta v_z = 4.6$  mm, in line with the design specifications of a  
 276 resolution better than 1% in momentum and 1 mrad in azimuthal angle [23].

277 **Scattering Electron** The efficiency of the CLAS12 trigger for DIS events,  
 278 with the electron scattered inside the acceptance at an energy above 1.5 GeV,  
 279 is greater than 99% [24]. Electrons are identified by a combination of signals  
 280 in the Cherenkov counters and calorimeters. Thanks to the large acceptance

281 of CLAS12, scattering electrons are detected in a wide kinematic range from  
 282 elastic events to DIS with an extended reach at large values of  $Q^2$ , Bjorken  $x$ ,  
 283 and forward hadron kinematics, see Fig. 3.

284 **Exclusive events** This can be a description how the forward detector can  
 285 be used to select exclusive events with the help of ML algorithms.

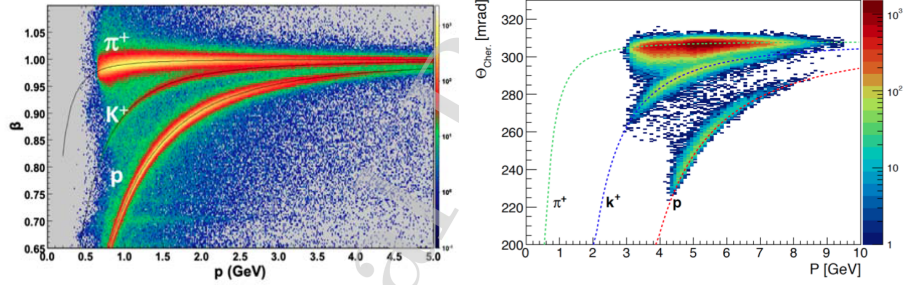


Fig. 4: (Left) The hadron separation provided by the Forward time-of-flight system. (Right) The hadron separation obtained by the RICH detector.

286 **Hadron PID** Identification of hadron particles is essential to gather flavor  
 287 information in SIDIS observables. The CLAS12 forward time-of-flight system  
 288 (FTOF) provides an excellent pion separation from kaons and protons at mo-  
 289 menta up to about 3 GeV/c and 5 GeV/c, respectively, see left panel of Fig. 4.  
 290 To complement such CLAS12 baseline configuration and provide hadron separa-  
 291 tion in the whole range of interest for SIDIS physics, up to momenta of 8  
 292 GeV/c, a ring-imaging Cherenkov detector (RICH) has been anticipated at the  
 293 time of the proposal. The RICH has been designed as composed by two mod-  
 294 ules in a left-right symmetric configuration, to reduce the systematic effects in  
 295 observables dependent on the target transverse polarization. The peculiar ge-  
 296 ometry of CLAS12 suggested an innovative hybrid-optics solution to limit the  
 297 active area to about 1 m<sup>2</sup> per sector, with part of the light directly imaged and  
 298 part of the light detected after reflection from mirrors. In order to limit the  
 299 material inside the acceptance and realize a light but stiff structure, composite  
 300 materials derived from aeronautic applications have been employed. Improve-  
 301 ments have been pursued in all the components, achieving the world leading  
 302 aerogel radiator clarity of 0.0050  $\mu\text{m}^4 \text{cm}^{-1}$  at high refractive index ( $n=1.05$ ),  
 303 a 20% reduction of the areal density of spherical mirrors in carbon fiber com-  
 304 posite polymer with respect the LHCb realization, the first use of glass-skin  
 305 planar mirrors in a nuclear physics experiment, the first use of the flat-panel  
 306 multianode H12700 photomultiplier with a dynode structure dedicated to the  
 307 single photon detection. The first module has been installed before the start  
 308 of CLAS12 data taking and the RICH completed in 2022 before the start of  
 309 the RGC polarized target run. Ongoing data analysis shows that the CLAS12  
 310 RICH is able to match the required time and Cherenkov angle resolutions, and

311 provide hadron separation in the wanted momentum range, see right panel of  
312 Fig. 4.

## 313 4.2 Luminosity

314 The CLAS collaboration has completed experimental runs with both liquid  
315 hydrogen and deuterium targets, and has reached the design luminosity of  
316  $10^{35} \text{ cm}^{-2}\text{s}^{-1}$  with a deuterium target and 45 nA electron beam current. This  
317 is much higher than the luminosity  $\mathcal{L} = 5 \times 10^{33} \text{ cm}^{-2}\text{s}^{-1}$  assumed for the RGH  
318 experiments. The ongoing high-lumi project aims to complement the CLAS12  
319 tracking with a front layer of micro-Rwell detectors, able to improve the spatial  
320 resolution and rate capability of CLAS12 tracking in the most critical region  
321 close to the interaction point, and support a factor two increase in luminosity.

322 With a dynamically polarized ammonia target, the luminosity is no longer  
323 limited by the target polarization lifetime, but by the background induced on  
324 the open-acceptance spectrometer. CLAS12 has measured the hit occupancy  
325 levels in the Drift Chambers (DC), the most sensitive detectors, as a function  
326 of the beam intensity and solenoid current. The typical occupancy is driven  
327 by Moeller scatterings in the target and secondary interactions in the shielding  
328 around the downstream beam pipe, in the detector structure and in the air  
329 filling the Hall. CLAS12 simulations reproduce data within an acceptable 30%  
330 level.

331 For the RGH experiments, where the CLAS12 solenoid is replaced by the  
332 target's 5 T transverse polarizing field, the Moeller background is no longer con-  
333 tained inside the beam pipe, but is mainly trapped inside the target region. The  
334 baseline of the RGH experiments is to run with no Forward Tagger (FT-OFF)  
335 and with additional shielding elements installed to minimize the secondary in-  
336 teractions.

337 The RGH background has an additional peculiar component, due to the  
338 energy loss of the beam particles passing without interaction through the target.  
339 If the loss is big enough, the particle is bent outside the pipe and into the  
340 detector acceptance. Such a background is concentrated in the bending plane  
341 of the 5T target magnet, creating the so-called *sheet-of-flame*. With a vertical  
342 magnetic field, the sheet-of-flame will illuminate sector 4 to a level that could be  
343 hardly sustainable with the present DC readout, able to record just a single hit  
344 in the extended readout gate (between  $0.5 \mu\text{s}$  and  $1.5 \mu\text{s}$  depending on the drift  
345 cell size). As a conservative approach, this work assumes to switch off sector  
346 4, and operate with the other 5 sectors up to a maximum tolerable occupancy  
347 rate of 4%. This corresponds to the design luminosity of  $5 \times 10^{33} \text{ cm}^{-2}\text{s}^{-1}$ .

348 With the addition of the micro-Rwell tracking layer under development for  
349 the CLAS12 high-lumi project, a significant improvement in luminosity is ex-  
350 pected. Possible mitigation measures can be introduced to partially operate  
351 sector 4. These includes switching off just the wires close to the beam where  
352 the background particles concentrate, veto the events with multiple particles as  
353 resolved by the high-lumi tracking layer, upgrade the DC readout to process  
354 multiple hits in the readout gate. All these developments are being pursued to

355 maximize the physics output of RGH experiments, with the possibility to over-  
 356 come what has been projected at the time of the proposal.

## 357 5 Physics Observables

358 Physics analyses are in progress based on the 12 GeV data. CLAS12 results for  
 359 both the SIDIS and exclusive channels have been published by the Collaboration  
 360 and presented at the conferences. As example, published beam spin asymmetry  
 361 of SIDIS  $\pi^+$ , SIDIS di-hadron and DVCS events, based on a fraction of the  
 362 recorder statistics, are shown in Fig. 5. Data confirm that CLAS12 allows a  
 363 much extended reach inside the DIS regime (large  $Q^2$ ) with respect CLAS and  
 364 the valence region (large  $x$ ) with respect previous experiments, with an unprece-  
 365 dented statistical precision. With the improved knowledge of the instrumental  
 366 effects, and the refinement of the calibration procedures and reconstruction algo-  
 367 rithms, further progresses are expected towards the best CLAS12 performance  
 368 before the start of RGH experiments.

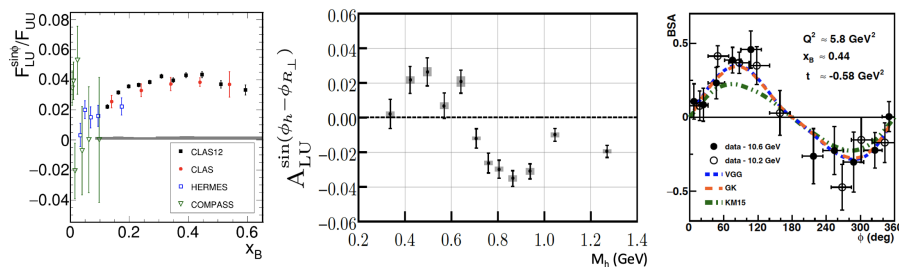


Fig. 5: CLAS12 published results on beam spin asymmetry observables based on just a fraction of the recorded statistics. SIDIS  $\pi^+$  asymmetry as a function of Bjorken  $x$  compared to previous results [32] (left), SIDIS di-hadron asymmetry find not-zero for the first time [33] (center), DVCS asymmetry as a function of the azimuthal angle  $\phi$  compared to phenomenological models [34] (right).

### 369 5.1 Semi-inclusive Physics

### 370 5.2 Exclusive Physics

## 371 6 Summary

372 In summary, the RGH experiments at CLAS12 offer a compelling physics pro-  
 373 gram that have the potential to provide unprecedented information on the pe-  
 374 culiar parton dynamics within the nucleon and during fragmentation. Since the  
 375 approval in 2012, the interest in this field of research has worldwide grown and

376 culminated with the recent EIC CD0 announcement, the theoretical understand-  
377 ing and lattice calculations have made important progresses and consolidate the  
378 interest in new experimental results. At the same time, a comprehensive pro-  
379 gram has been pursued at JLab to understand and overcome the technical chal-  
380 lenges connected with running a transversely polarized target inside CLAS12,  
381 and only external conditions have temporarily delayed its accomplishment.

## 382 References

- 383 [1] H. Avakain et al., *Transverse spin effects in SIDIS at 11 GeV with a transversely*  
384 *polarized target using the CLAS12 Detector*.  
385 [https://www.jlab.org/exp\\_prog/proposals/12/C12-11-111.pdf](https://www.jlab.org/exp_prog/proposals/12/C12-11-111.pdf).
- 386 [2] H. Avakain et al., *Measurement of transversity with dihadron production in SIDIS*  
387 *with transversely polarized target*.  
388 [https://www.jlab.org/exp\\_prog/proposals/12/PR12-12-009.pdf](https://www.jlab.org/exp_prog/proposals/12/PR12-12-009.pdf).
- 389 [3] H. Avakian et al., *Deeply Virtual Compton Scattering at 11 GeV with transversely*  
390 *polarized target using the CLAS12 Detector*.  
391 [https://www.jlab.org/exp\\_prog/proposals/12/PR12-12-010\\_rv.pdf](https://www.jlab.org/exp_prog/proposals/12/PR12-12-010_rv.pdf).
- 392 [4] PAC39 Report,  
393 [https://www.jlab.org/exp\\_prog/PACpage/PAC39/PAC39%20Final.Report.pdf](https://www.jlab.org/exp_prog/PACpage/PAC39/PAC39%20Final.Report.pdf).
- 394 [5] PAC42 High-Impact Selection,  
395 [https://www.jlab.org/exp\\_prog/PACpage/High\\_Impact.Proposals.pdf](https://www.jlab.org/exp_prog/PACpage/High_Impact.Proposals.pdf).
- 396 [6] A. Accardi et al., *Electron Ion Collider: The Next QCD Frontier : Understanding*  
397 *the glue that binds us all*, Eur.Phys.J.A 52 (2016) 9, 268.
- 398 [7] H. Avakian, A. Bressan and M. Contalbrigo, *Experimental results on TMDs*, Eur.  
399 Phys. J. A52 (2016) 6, 150.
- 400 [8] M. Pitschmann et al., *Nucleon tensor charges and electric dipole moments*, Phys.  
401 Rev. D91 (2015) 074004.
- 402 [9] A. Courtoy et al., *Beyond-Standard-Model Tensor Interaction and Hadron Phe-*  
403 *nomenology*, Phys. Rev. Lett. 115 (2015) 162001.
- 404 [10] C. Alexandrou, *Recent progress on the study of nucleon structure from lattice*  
405 *QCD and future perspectives*, SciPost Phys. Proc. 3 (2020) 015.
- 406 [11] A. Bacchetta et al., *Matches and mismatches in the descriptions of semi-inclusive*  
407 *processes at low and high transverse momentum*, JHEP 08 (2008) 023.
- 408 [12] M. Radici and A. Bacchetta, *First Extraction of Transversity from a Global Anal-*  
409 *ysis of Electron-Proton and Proton-Proton Data*, Phys.Rev.Lett. 120 (2018) 19,  
410 192001.
- 411 [13] I. Garzia and F. Giordano, *Transverse-momentum-dependent fragmentation func-*  
412 *tions in  $e^+e^-$  annihilation*, Eur. Phys. J. A52 (2016) 6, 152.

- 413 [14] M.J. Skoby, *High Precision Measurement of Transversity Using Di-hadron Cor-*  
414 *relations in  $\vec{p}-p$  Collisions at  $s_{NN} = 500$  GEV.*, Int. J. Mod. Phys. Conf. Ser.  
415 40 (2016) 1660038.
- 416 [15] L. Adhikari and M. Burkardt, *Angular Momentum Distribution in the Transverse*  
417 *Plane*, Phys. Rev. D94 (2016) 11, 114021.
- 418 [16] N. d'Hose, S. Niccolai and A. Rostomyan, *Experimental overview of Deeply Vir-*  
419 *tual Compton Scattering*, Eur. Phys. J. A52 (2016) 6, 151.
- 420 [17] A. Honig, *Highly Spin-Polarized Proton Samples – Large, Accessible, and Simply*  
421 *Produced*, Phys. Rev. Lett. 19 (1967) 1009.
- 422 [18] S. Hoblit et al., *Measurements of  $\vec{HD}(\vec{\gamma}, \pi)$  and Implications for the Convergence*  
423 *of the Gerasimov-Drell-Hern Integral*, Phys. Rev. Lett. 102, 172002 (2009).
- 424 [19] D. Ho et al., *Beam-Target Helicity Asymmetry for  $\vec{\gamma} \vec{n} \rightarrow \pi^- p$  in the  $N^*$  Reso-*  
425 *nance Region*, Phys. Rev. Lett. 118, 242002 (2017).
- 426 [20] Kevin Wei, *The Response of Polarized Protons in Solid Hydrogen-Deuteride*  
427 *(HD) to Electron Beams*, Ph.D. Thesis, University of Connecticut (2021).
- 428 [21] C.D. Keith, *Polarized Solid Targets at Jefferson Lab*, Proceedings of  
429 PSTP2015, The XVI International Workshop in Polarized Sources, Tar-  
430 gets, and Polarimetry, PoS(PSTP2015)013.
- 431 [22] J. Pierce et al., *Dynamically polarized target for the and  $g_2^p$  and  $G_E^p$  exper-*  
432 *iments at Jefferson Lab*, Nucl. Instr. Meth. Phys. Res. A 738, 54 (2014).
- 433 [23] V.D. Burkert et al., *The CLAS12 Spectrometer at Jefferson Laboratory*,  
434 Nucl. Instrum. Meth. Phys. Res. A 959 (2020) 163419.
- 435 [24] B. Raydo et al., *The CLAS12 Trigger System*, Nucl. Instrum. Meth. Phys.  
436 Res. A 960 (2020) 163529.
- 437 [25] M. Contalbrigo et al., *The CLAS12 Ring Imaging Cherenkov detector*, Nucl.  
438 Instrum. Meth. Phys. Res. A 964 (2020) 163791.
- 439 [26] D. Frankel, *Model for flux trapping and shielding by tubular superconducting*  
440 *samples in transverse fields*, IEEE Trans. Magn. 15 (1979) 1349.
- 441 [27] J. F. Fagnard et al., *Magnetic shielding properties of a superconducting*  
442 *hollow cylinder containing slits: modeling and experiment*, Supercond. Sci.  
443 Technol. 25 (2012) 104006.
- 444 [28] K. Vinod, R. G. Abhilash Kumar and U. Syamaprasad, *Prospects for MgB<sub>2</sub>*  
445 *superconductors for magnet application*, Supercond. Sci. Technol. 20 (2007)  
446 R1.
- 447 [29] J.J. Rabbers et al., *Magnetic shielding capability of MgB<sub>2</sub> cylinders*, Su-  
448 percond. Sci. Technol. 23 (2010) art. n. 125003.

- 
- 449 [30] M. Statera et al., *A bulk superconducting magnetic system for the CLAS12*  
450 *target at Jefferson Lab*, IEEE Trans. Appl. Supercond. 115 (2015) art. n.  
451 4501004.
- 452 [31] M. Statera et al, *Magnetic System for the CLAS12 Proposals*, IEEE Trans.  
453 Appl. Supercond. 23 (2013) art. n. 3800304.
- 454 [32] S. Diehl et al. (CLAS12), *Multidimensional, High Precision Measurements*  
455 *of Beam Single Spin Asymmetries in Semi-inclusive  $\pi^+$  Electroproduction*  
456 *off Protons in the Valence Region*, Phys. Rev. Lett. 128 (2022) 6, 062005.
- 457 [33] T.B. Hayward et al. (CLAS12), *Observation of Beam Spin Asymmetries*  
458 *in the Process  $ep \rightarrow e' \pi^+ \pi^- X$  with CLAS12*, Phys. Rev. Lett. 126 (2021)  
459 152501.
- 460 [34] G. Christiaens et al. (CLAS12), *First CLAS12 Measurement of Deeply Vir-*  
461 *tual Compton Scattering Beam-Spin Asymmetries in the Extended Valence*  
462 *Region*, Phys. Rev. Lett. 130 (2023) 21, 211902.